



## New model for an epoxy-based brachytherapy source to be used in spinal cancer treatment

José T. Silva, Carla Daruich de Souza<sup>\*</sup>, Lucas Verdi Angelocci, Wilmmmer Alexander Arcos Rosero, Beatriz Ribeiro Nogueira, Ruanyto Willy Correia, Carlos Alberto Zeituni, Maria Elisa Chuery Martins Rostelato

Laboratório de Produção de Fontes para Radioterapia, Instituto de Pesquisas Energéticas e Nucleares (IPEN / CNEN - SP), Universidade de São Paulo, Av. Professor Lineu Prestes 2242, 05508-000, São Paulo, SP, Brazil

### ARTICLE INFO

#### Keywords:

CNS cancer  
Phosphorus-32  
Brachytherapy  
Epoxy radiation source  
mcnp dose simulation

### ABSTRACT

The present work described the cold fabrication of a P-32 radioactive source to be used in CNS cancer using epoxy resin. The epoxy plaque fabricated with Teflon mold presented better agreement. MCNP simulation evaluated the radiation dose. Special attention was given to factors that can impact dose distribution. Average dose was  $16.44 \pm 2.89\%$  cGy/s. Differences of less than 0.01 cm in thickness within the plaque lead to differences of up to 12% in the dose rate.

### 1. Introduction

With the steady growth in the number of patients around the world, new and efficient forms of cancer treatment are in high demand. It is also important that these new treatments are locally produced resulting in lower cost and ultimately becoming available for more patients. Among the possible treatments, brachytherapy is a strong contender. By placing radioactive seeds directly inside the cancer, it is possible to better achieve the major goal of radiation therapy: focusing the effects of radiation in the target saving the healthy surrounding tissues.

Fabricating a new radioactive source in a semi-industrial scale is not easy task. Several steps must be fulfilled before even handling radioactive material. Usually, the initial prototype is fabricated without radioactive material to ensure high yields in the chemical and/or mechanical assembly. After a route is determined, optimization of each step is still performed with no radioactive material. This assures a good start point condition for radioactive tests. These initial tests are important because crucial steps such as concentrations, selection of the best tools, set ups, and others can all be determined without the presence of radiation assuring operator safety and avoiding unnecessary wastes (Daruich de Souza et al., 2021). The constraints for manufacture in large scale are

many, but the final product might be the only and/or the best treatment available. Also, dose simulations are performed simultaneously, since it can greatly impact fabrication steps. For example, simulation can quantify how much a variant parameter is impacting radiation dose distribution and, ultimately, if something can be done to mitigate it.

The central nervous system (CNS) is formed by the brain and spinal cord. CNS cancer can be developed on the brain, cranial nerves, meninges, or on the spinal cord itself (Nabors et al., 2013). Tumor resection in the spinal or cerebral region is a risk due to the proximity of the tumor to the dura, in addition to putting the patient at risk for possible neurological diseases (Nabors et al., 2013). Due to the complexity of the site, low dose radiotherapy has been used post-operatively in local recurrences (Pandey et al., 2006). Patients with this tumor type experience a high degree of suffering due to a possible compression of the spinal cord and the numerous sequels that may occur, mainly because the disease affects regions that control the motor activity (Nabors et al., 2013). One of the main issues with cancer removal surgeries in the CNS is the possibility of recurrence (Nabors et al., 2013; Regine et al., 2002).

Phosphorus-32 is one of the many radioisotopes to be used in medicine. It is one of the first bone-seeking radioisotopes (Ziessman et al.,

<sup>\*</sup> Corresponding author. Laboratório de Produção de Fontes para Radioterapia, Instituto de Pesquisas Energéticas e Nucleares (IPEN / CNEN - SP), Universidade de São Paulo, Av. Professor Lineu Prestes 2242, 05508-000, São Paulo, SP, Brazil.

E-mail addresses: [tiagofisicausp@gmail.com](mailto:tiagofisicausp@gmail.com) (J.T. Silva), [cdsouza@ipen.br](mailto:cdsouza@ipen.br), [carladdsouza@yahoo.com.br](mailto:carladdsouza@yahoo.com.br) (C. Daruich de Souza), [lucasangelocci@usp.br](mailto:lucasangelocci@usp.br) (L.V. Angelocci), [arcosquim@gmail.com](mailto:arcosquim@gmail.com) (W.A. Arcos Rosero), [bia.ribnog@gmail.com](mailto:bia.ribnog@gmail.com) (B.R. Nogueira), [ruanyto@usp.br](mailto:ruanyto@usp.br) (R.W. Correia), [czeituni@ipen.br](mailto:czeituni@ipen.br) (C.A. Zeituni), [elisaros@ipen.br](mailto:elisaros@ipen.br) (M.E. Chuery Martins Rostelato).

<https://doi.org/10.1016/j.apradiso.2021.109952>

Received 21 February 2021; Received in revised form 25 August 2021; Accepted 13 September 2021

Available online 22 September 2021

0969-8043/© 2021 Elsevier Ltd. All rights reserved.

2014). For example, in 2006 some bandages incorporating phosphorus-32 were used on treatment of superficial tumors (Pandey et al., 2006). It can be used to differentiate choroidal hemangiomas from other malignant choroidal tumors (Sanborn, 2006). With its high beta energy of 695.03 keV (1710.66 keV max) and 14.27 days of half-life, this isotope is ideal to treat spinal cancer in the intra-operative mode (Meyerhof, 1989; Podgorsak, 2005).

Spinal brachytherapy with Phosphorus-32 was first described by William Y. Tong et al. (2014) in 2012. One patient underwent an intraoperative brachytherapy session using a plaque with phosphorus-32, delivering a total dose of 10 Gy during a treatment that lasted 13 min and 28 s. This type of therapy proved to be effective, because further examinations showed that there was no evidence of recurrences. Prior to that, Yamada et al. (2005) incorporated phosphorus-32 in a flexible film and used it to treat dura mater contaminated with residual tumor cells from CNS cancer. The film, approximately 0.35 mm, delivered a dose of 1 Gy/min to the treated surface after surgery. Phosphorus-32 brachytherapy combined with advanced Image Guided Radiation Therapy results in less radiation for the patient, when compared to classical techniques. In 2015, a study was performed by Folkert et al. (Folkert et al., 2015) with 68 patients presenting malignant tumors in the spine region. Silicone plaques containing phosphorus-32 were used effectively in intraoperative treatment.

Our group in Brazil is developing this new source for CNS treatment (Benega et al., 2012, 2013). The present work describes the cold fabrication of the source in plaque form using epoxy resin, paying special attention to factors that can greatly impact dose distribution. At the end, a MCNP4C Monte Carlo simulation was used to evaluate the dose profile of the plaque and a dose curve in function of plaque thickness.

## 2. Methodology

Before starting the radioactive fabrication of the treatment plaque, it is necessary to develop a mold that needs to:

- Receive the material without reacting with it;
- Preferably be re-useable;
- Have an easy release: the radiation source can be removed without ripping.

## 3. Epoxy resins

Epoxy resins (ER) are classified under the name of ethoxylated resins. These resins, which are produced by the condensation of bisphenol A and epichlorohydrin, contain terminal epoxy groups and may contain many hydroxyl pendant groups, depending on molecular weight. Generally, ERs are not used alone for coatings, normally being cross-linked. Epoxy resins, based upon bisphenol A (or F) and epichlorohydrin, cured at room temperature by aliphatic polyfunctional amines and polyamides, are used in heavy duty coatings for ships, oil rigs, and storage tanks, as well as water pipes. Commonly used aliphatic amine hardeners permit room temperature cure, but the reaction is strongly exothermic, causing problems in thick moldings. Aromatic amine hardeners require higher curing temperatures but are better suited to large parts and give relatively high heat deflection temperatures (up to 230 °C). Anhydride hardeners are less toxic and less polar than amines, but need an accelerator. With suitable catalysis, ERs may also be cured thermally or photolytically without a co-reagent (Ehlers et al., 2007; Giannotti et al., 2003; Gooch, 2011; Ignatenko et al., 2020; Konuray et al., 2017; Oldring, 2003; Vidil et al., 2016).

## 4. Materials used: resin and catalyst

The resin SQ2220 is a low viscosity epoxy resin combining the performance properties of standard bisphenol A epoxy resin with the low

viscosity of bisphenol F epoxy resin. The composition is (Blackburn Electric Wires, 2012):

- Bisphenol A/F epoxy resins Mw < 700;
- Butanedioldiglycidyl ether;
- Epoxy phenol novolac resin.

The Catalyst SQ3154 is a low viscosity modified Cycloaliphatic Amine hardener that reacts with epoxy resins to form thermosetting systems. Has low exotherm (Oliveira et al., 2020).

The SQ2220 resin combines the properties of the types of resins widely used in the industry, the bisphenol A BPA is a nonsteroid synthetic chemical compound and belongs to the bisphenol group of compounds with two hydroxyphenyl groups; and the bisphenol F BPF a small aromatic organic compound. It is related to bisphenol A through its basic structure, as both belong to the category of molecules known as bisphenols, which feature two phenol groups connected via a linking group, that explains its high compatibility (Rochester and Bolden, 2015). In the case of BPA, due to their chemical structure and cross-linking properties, BPA has been extensively used in the manufacture of polycarbonate plastics, epoxy resins, and thermal paper. As BPA has intrinsic heat resistance and elasticity, its use has progressively increased (Vandenberg, 2014). The BPF is used in the manufacturing of plastics and epoxy resins. It is used in the industry as a way of increasing the thickness and durability of materials (Rochester and Bolden, 2015).

Thus, the mixture of BPA and BPF resins produces the SQ2220 resin, which as a commercial resin that synergistically combines physical and chemical properties. Due to its low cost, application is highly feasible, and a large number of samples can be made.

Epoxy resins are often divided into two types: those cured at low (room) temperature and at elevated temperatures. The most widely used low-temperature hardeners include polyamide and amidoamine curing agents as well as aliphatic amines (such as diethylenetriamine, triethylenetetramine, and their derivatives), catalytic amines (e.g., dimethylaminomethyl phenol), sulphur-containing curing agents (mercaptans), and amine adducts. Although room temperature curing epoxy resins are very convenient in many applications.

Aliphatic amine, which rapidly reacts with epoxy resin, is a representative room-temperature curing agent. Resins that have been cured using aliphatic amines are strong, and are excellent in bonding properties. They have resistance to alkalis and some inorganic acids, and have good resistance to water and solvents (Gooch, 2011). Thus, the choice of the catalyst was taken into account due to its chemical characteristics.

## 5. Molds

### 5.1. Polytetrafluoroethylene

PTFE polymers, such as Teflon, is an example of a linear fluoropolymer. Formed by the polymerization of tetrafluoroethylene (TFE), the (CF<sub>2</sub>CF<sub>2</sub>) groups repeat many thousands of times. The fundamental properties of fluoropolymers evolve from the atomic structure of fluorine and carbon and their covalent bonding in specific chemical structures. The PTFE molecule is simple and is highly ordered and can align itself with other molecules or other portions of the same molecule. Disordered regions are called amorphous regions. Again, polymers with high crystallinity require more energy to melt presenting higher melting points (Ebnesajjad, 2011). PTFE has excellent chemical resistance, a wide working temperature range (−260 to 260 °C) and a small friction coefficient, which allows the materials it holds to be removed easily. It is also an inert material (BENTO, 2011).

### 5.2. Polydimethylsiloxane (PDMS)

Polydimethylsiloxane (PDMS), also known as silicone, is a material commonly used in various fields for decades: from microfluidic to

fabrication of biomedical implantable devices (Contact lenses, cochlear implants, urinary catheters, breast implants). Silicone material exhibits great properties. It is highly permeable to gases, optically transparent, and easy to manufacture. The material has excellent mechanical properties (flexible) and low-cost. For the use in the biomedical field, the material is biocompatible and has low-toxicity. Is characterized by its siloxane backbone. Silicone material is known to be inert, which makes it not easily oxidizable and degraded by environmental factors like humidity, oxidation, temperature variation, and chemically inert (Lam et al., 2020; Liravi and Toyserkani, 2018). In addition, it is a malleable material resulting in an easy release (CASTRO, 2008; Ignatenko et al., 2020). The molecular structure of both materials is shown in Fig. 1.

### 5.3. Set up

The first option was a commercial silicone mold (Fig. 2) from the PrimeChef Company, with dimensions of  $7.50 \times 7.50 \text{ cm} \pm 0.05$  with  $2.0 \text{ cm} \pm 0.05$  depth.

The second option was a Teflon mold (Fig. 3) with  $5 \text{ mm} \pm 0.0005$  of thickness,  $5.00 \times 5.00 \text{ cm} \pm 0.05$ .

The epoxy plaques are manufactured from mixture of the resin SQ2220, with density  $1.11 \pm 0.02 \text{ g/cm}^3$  at  $25^\circ\text{C}$ , and catalyst SQ3154, with density  $1.010 \pm 0.005 \text{ g/cm}^3$ , both from the company Silaex (São Paulo, Brazil). The proportion was 2: 1 in mass of resin and catalyst, respectively.

To simulate the radioactive material, HCl was added at a concentration of 2%. The HCl (ProQuímicos, analytic purity grade, 37%) was used to simulate phosphorus-32, since it is the same vehicle used in the radioactive material. The amount of HCl was 5% of the total mass value of the resin and catalyst mixture.

First, the mass of the catalyst and HCl was measured in separate flasks. Afterwards, these two products were manually mixed with borosilicate glass spatula for a period of 1 min. Then, the resin was added. The ready mix was placed in the silicone mold that had the pre-established tare. Were used:  $26.35 \text{ g} \pm 0.005$  of resin,  $13.44 \text{ g} \pm 0.005$  of catalyst and  $1.92 \text{ g} \pm 0.005$  of HCl. Six samples were produced with 5 g each, identified as: A1, A2, A3, A4, A5 and A6. The experiment was put to rest at rt for a period of 24 h to cure the resin. The surface on which the experiments were carried out was leveled to ensure a straight surface condition.

The Teflon mold received 4 g of the mixture: resin, catalyst, and HCl, with the proportion of each element mentioned above. The amount of HCl was 10% over the total mass of resin and catalyst. After the mixture was poured in the plaque, they were flattened by an epoxy spatula. Five samples were produced with these parameters.

### 5.4. Monte Carlo simulation parameters

This work used Monte Carlo method transport code MCNP4C to evaluate dose distribution at a radiochromic film in contact with the radioactive plaque, for future comparisons with experimental data to be obtained. Three different cases were simulated:

- a homogeneous plaque with a nominal thickness to evaluate dose homogeneity in ideal conditions of manufacturing;

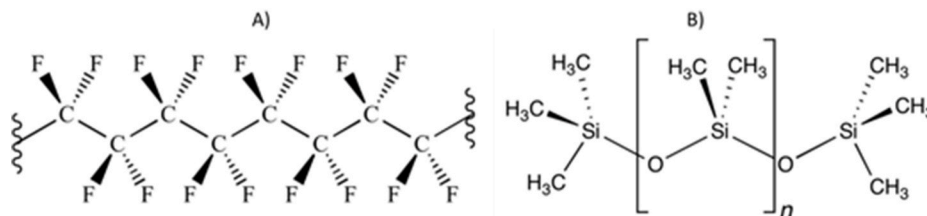


Fig. 1. Molecular structure of A) Teflon and B) Silicone.



Fig. 2. Silicon mold. (For interpretation of the references to colour in this figure legend, the reader is referred to the Web version of this article.)

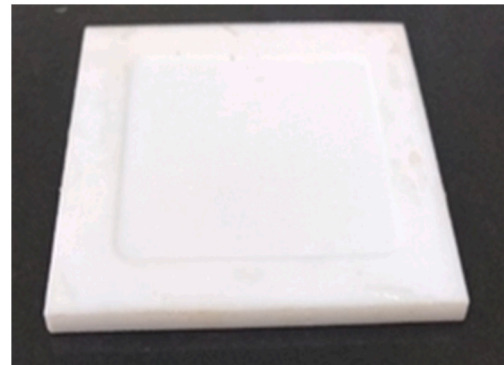
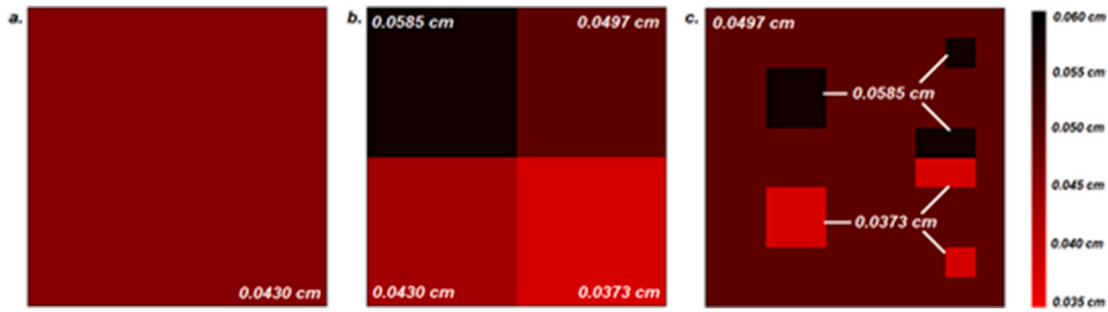


Fig. 3. Teflon mold.

- a heterogeneous plaque divided in four quadrants with different thicknesses to evaluate impact on dose by variation on thickness;
- a heterogeneous plaque with specific regions with different thicknesses to evaluate how different sizes of heterogeneities would impact final dose.

All plaques are  $5 \times 5 \text{ cm}^2$  and dose was calculated in the region of same dimensions right below the plaque, in the active layer of the film, to analyze homogeneity in the region of interest for clinical practice. Dose distribution around the borders of the plaque or beyond are estimated to be very low in relation to the region of interest due to low beta radiation penetration and were not subject of this work. Fig. 4 shows the simulation setup for the three simulated cases. Criteria for selecting thickness was related to results obtained in the manufacturing of the plaque and are explained further in the text, in the results section.

Additionally, MCNP4C code was used to define a polynomial that could describe variation on dose rate in function of thickness. For this, five different simulations were executed considering homogeneous plaques of thickness  $0.02 \text{ cm}$ – $0.06 \text{ cm}$  in  $0.01 \text{ cm}$  steps. MATLAB® software was used to process data and to find the best polynomial to fit the data.



**Fig. 4.** Simulation setup for three cases: a) Homogeneous plaque with nominal thickness; b) Heterogeneous plaque divided in four quadrants with different thicknesses; c) Heterogeneous plaque with localized heterogeneities in different areas.

In accordance to the American Association for Physicists in Medicine’s report TG-268 (Rogers et al., 2018) Table 1 presents the parameters used in this simulation, while Table 2 presents the considered material composition.

**Table 1**  
Monte Carlo simulation data following TG-268 report (Rogers et al., 2018).

Item	Description and References
Software	MCNP4C (BRIESMEISTER, 2002)
Hardware	7th gen Intel® dual core i5-7200U processor with 8 GB RAM (clock speed of 2.5 GHz). Total simulation time for the first three cases was around 60 h, and for the five simulations to calculate polynomial around 43 h.
Geometry	Source in plaque format centered in origin, with dimensions of $5 \times 5 \text{ cm}^2$ , placed over a $10 \times 10 \times 0.0278 \text{ cm}^3$ EBT3 radiochromic film, both within a $10 \times 10 \times 10 \text{ cm}^3$ water phantom. The radiochromic film is composed of three layers: two external ones with thickness of 0.0125 cm and the active layer in between then, with thickness of 0.0028 cm. Thickness of plaque was varied in each simulated case according to Fig. 4.
Materials	The material atomic composition for the plaque was estimated from the composition of the reagents used. In some cases, the composition was not fully described even contacting the producers (industrial secret). In these cases, its atomic composition was supposed to be proportional to the known part. See Table 2 for materials and reference.
Source	<ul style="list-style-type: none"> <li>• A total of <math>10^8</math> particle-stories were simulated for each of the first three cases. The five simulations to define the polynomial fit were run with <math>3 \times 10^7</math> particle-stories each.</li> <li>• All volume of the plaque was considered as a source. Beta emission spectra was taken from literature. (INTERNATIONAL ATOMIC NUCLEAR AGENCY, 2019)</li> </ul>
Physics and Transport Scoring	<ul style="list-style-type: none"> <li>• Default cross-section libraries, particle weight and energy cutoffs from MCNP4C were used.</li> <li>• Tally F6 was used to estimate average energy deposited in medium;</li> <li>• Tally was scored in sections of <math>0.5 \times 0.5 \times 0.0028 \text{ cm}^3</math> of the active layer of the film, in a grid of <math>10 \times 10</math> sections;</li> <li>• Type-A uncertainty obtained from MCNP4C was below 0.3% for any scored section for the three cases studied and for the simulations to calculate the polynomial fit.</li> </ul>
Analysis	Scored quantities were not filtered. Data was obtained as dose (in MeV/g) by particle. Since the intended activity of the plaque is around 300 mCi ( $1.11 \times 10^{10}$ Bq) for clinical practice, the result obtained was multiplied by this number of particles, then converted to J/kg to be presented as dose rate in multiple of the Gy unit per time. Simulations done to calculate the polynomial fit, however, are presented in function of the activity.
Validation	This work aimed to use MCNP4C as a mean to estimate dose distribution by this source under the presented conditions of manufacturing. Validation of this simulation by comparison with data obtained from experiments with EBT3 radiochromic film is subject of a future work.

**Table 2**  
Material compositions used in MCNP4C simulations.

Material	Atomic composition	Density (g/cm <sup>3</sup> )	Source
Plaque	H: 53.0% C: 39.1% O: 6.8% N: 1.1%	0.786	Estimated from the composition of reagents used.
EBT3 coating	H: 36.4% C: 45.5% O: 18.2%	1.35	Palmer et al. (2015)
EBT3 active layer	H: 56.8% C: 27.6% O: 13.3% Al: 1.6% Li: 0.6%	1.20	Palmer et al. (2015)
Water	H <sub>2</sub> O: 100%	0.98	–

## 6. Results

### 6.1. Experimental

The epoxy plaques obtained from the silicone and Teflon molds had their thicknesses measured with a digital micrometer with a precision of  $0.001 \text{ mm} \pm 0.0005$ .

The measurements were performed at different points on the plaque, as well as averages and respective standard deviations were calculated. Results are presented in Tables 3 and 4.

The epoxy plaque fabricated with the silicone mold yield a high degree of variation in thickness uniformity. As show in Table 3, the sample A6 had a variation of more than 0.600 mm. This factor when the radioactive material is immobilized on the plaque can cause a problem, because it causes significant dose shifts (as proven in MCNP calculations).

**Table 3**  
Thickness measurements from silicone mold.

Samples	A1	A2	A3	A4	A5	A6
Measurements (mm) ± 0.0005	0.771	0.582	0.657	0.625	0.646	0.699
	0.807	0.609	0.747	0.709	0.576	0.845
	0.761	0.765	0.637	0.701	0.476	0.934
	0.712	0.686	0.591	0.663	0.357	0.835
	0.785	0.723	0.629	0.657	0.823	0.733
	0.773	0.681	0.796	0.724	0.844	0.433
	0.723	0.802	0.819	0.770	0.797	0.922
	0.602	0.765	0.778	0.707	0.743	0.821
	0.586	0.815	0.742	0.717	0.803	0.464
	0.582	0.811	0.802	0.771	0.475	0.298
	0.492	0.702	0.777	0.780	0.657	0.425
	0.496	0.580	0.613	0.746	0.704	0.738
	0.444	0.718	0.685	0.592	0.775	0.540
Average	0.656	0.710	0.713	0.704	0.667	0.668
Standard Deviation	0.127	0.082	0.080	0.057	0.155	0.211

**Table 4**  
Thickness measurements from Teflon mold.

Samples	A	B	C	D	E	
Measurements (mm) $\pm$ 0.0005	0.296	0.371	0.504	0.400	0.367	
	0.316	0.317	0.465	0.454	0.360	
	0.324	0.285	0.405	0.373	0.363	
	0.267	0.328	0.494	0.436	0.344	
	0.310	0.373	0.454	0.484	0.348	
	0.338	0.394	0.408	0.517	0.350	
	0.359	0.355	0.475	0.517	0.351	
	0.336	0.292	0.452	0.540	0.344	
	0.321	0.292	0.397	0.557	0.325	
	0.306	0.286	0.394	0.538	0.315	
	0.270	0.345	0.433	0.585	0.299	
	0.278	0.374	0.452	0.550	0.320	
	0.280	0.410	0.458	0.451	0.366	
	0.260	0.398	0.446	0.514	0.350	
	0.260	0.362	0.461	0.537	0.353	
	Average	0.301	0.345	0.447	0.497	0.344
	Standard Deviation	0.031	0.043	0.034	0.062	0.020

Greater thickness indicates a higher concentration of material, consequently, this will lead to a higher concentration of radioactive material. Less thickness, less material concentration. Thus, the dose distribution will not be uniform.

Epoxy plaques from the Teflon mold presented better agreement. Samples A, B and E, with respective values of average thickness (mm): 0.301, 0.345, and 0.344. There are also interesting values for samples C and D with respective values of average thickness (mm): 0.447 and 0.497.

Comparing the thickness variations between the plates of the different molds, the advantage of using Teflon is notable. The standard deviation of the Teflon mold was smaller, crediting a more uniform plaque, without great variations in thickness.

The molecular structures of the polymers (Fig. 1) can provide a possible explanation. Silicone is a more malleable material; polysiloxanes differ from other polymers in that their backbones consist of Si–O–Si units unlike many other polymers that contain carbon backbones. Polysiloxane is very flexible due to large bond angles and bond lengths when compared to those found in more basic polymers such as polyethylene. For example, a C–C backbone unit has a bond length of 1.54 Å and a bond angle of 112°, whereas the siloxane backbone unit Si–O has a bond length of 1.63 Å and a bond angle of 130°. Polymer segments can move farther and change conformation easily, making for a flexible material. Polysiloxanes tend to be more stable and less chemically active because more energy is required to break the silicon-oxygen bond (Shinetsu *Silicone*, 2020). On account of this the bottom of the mold cannot be completely flat. Teflon the backbone is formed of carbon-carbon bonds and the pendant groups are carbon-fluorine bonds. Both are extremely strong bonds, as a result of its strong and inflexible chemical structure, a sufficiently firm mold is obtained to reduce the variations in the plates produced (Ebnesajjad, 2011).

## 7. Monte Carlo simulation

Criteria for defining the thickness of the plaques for simulation are presented here. For the first case, the nominal value of 0.043 cm was used because it represents the average value obtained on a large batch measured, and was considered a desirable thickness. The second and third cases presented in Fig. 4 were based on results shown in Table 4, where average, minimum and maximum values for sample D were taken. Sample D was chosen because it presented the largest standard deviation of thicknesses measured, thus values were extracted from it to assure a larger coverage of possible cases. The second case used a plaque divided in quadrants, three using these values from sample D and one with the nominal value of 0.043 cm. This configuration allows dose rate to be compared in large regions with all different thickness values

analyzed. The third case simulates a plaque with the average thickness value of sample D and heterogeneities of different sizes spread through the plaque, both at the minimum and maximum thickness value, to evaluate how they would impact dose around it. Fig. 5 shows the dose profile obtained from the Monte Carlo simulations following parameters presented in Table 1, in each of the three cases presented in Fig. 4.

The first noticeable aspect seen in Fig. 5 is that all three cases simulated showed a similar behavior in the outer scoring sections of the grid. This behavior is expected because there is an escape of scattered electrons which is not compensated by the income of electrons, i.e., there is no electronic equilibrium near the borders of the plaque. The dose to these sections is also lower by geometrical reasons, since the source ends at those regions, while in the central area the active plaque contributes to dose with electrons from all neighboring points beyond the directly aligned to it.

Average dose obtained for the homogenous plaque was  $16.44 \pm 2.89\%$  cGy/s, or  $16.97 \pm 2.26\%$  cGy/s discarding the outer regions, to estimate dose only in the central area. Dose in each section of the scored grid was within the interval of 14.35–17.08 cGy/s, or 16.85–17.08 cGy/s discarding the outer regions, which is a variation of less than 1.4% from the lowest to highest dose scored. Since there is an overall agreement of dose in each section, with a very small deviation, MCNP4C was successfully used to estimate that the plaque in the presented configuration is able to deliver a homogeneous dose in the region of interest for treatment as long as homogeneous thickness is obtained in the manufacturing process.

The dose profile presented in Fig. 5b shows very distinct dose values in each of the four quadrants, but the sections of the grid in the borders between each region show a slight difference from the rest of the quadrant. Influence of scattered radiation from a region of different thickness seems to impact dose in these sections. To better evaluate impact of heterogeneities, the third case simulated regions of different thickness. By comparing Figs. 4 and 5 it is visible that the presence of heterogeneities affects directly the dose in the tissue right in contact with the source, but is also visible that neighboring regions of the film suffered a tilt on dose, which indicates that the mean range of electrons in the material is higher than the scoring grid resolution (0.5 cm). Continuous slowing down approximation range for electrons in water for the phosphorus-32 average emission energy is around 0.28 cm, and for the maximum energy is around 0.84 cm (National Institute of Standards and Technology, 2020). This information and the behavior visible on Fig. 5c indicate that heterogeneities present on the plaque impact dose mainly in regions of the target tissue very near to the heterogeneity location; still, since differences of less than 0.01 and 0.02 cm in thickness within the plaque, which were noted on the actual manufactured plaques, lead to differences of up to 12% and 40% in the dose rate, respectively, it is highly recommended that the plaque be manufacture as homogeneous as possible. Although these results are obtained for the quadrant plaque (Fig. 5b), therefore for larger areas with thickness variation, Fig. 5c shows that even small area heterogeneities still lead to differences of 25% if this variation is abrupt.

To account for the impact on dose of possible variations on thickness, five other Monte Carlo simulations were executed, considering homogeneous plaques with thickness varying from 0.02 to 0.06 cm. A second-degree polynomial fit (Equation (1)) was calculated using MATLAB®, with a norm of residuals of 0.0025, a good agreement with data obtained from simulation. The fitting parameters uncertainty boundaries (95% confidence) are  $\pm 20.61$  for the quadratic coefficient,  $\pm 1.66$  for the linear coefficient and  $\pm 0.03$  for the constant term.

$$\dot{D}(t, A) = (129.94t^2 - 29.97t + 4.86) * 10^{10} \frac{cGy}{s Bq} \quad (1)$$

Equation (1) was obtained considering the thickness range of 0.2–0.6 cm and can be used to estimated variations on dose range for plaques manufactured with different thickness. With further study, including comparisons with experimental data, this information can be

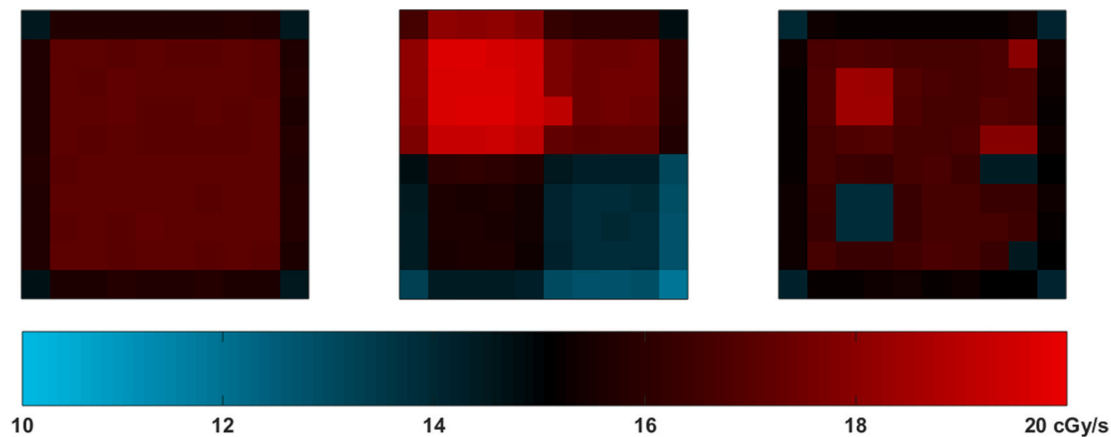


**Fig. 5.** Dose simulated with MCNP4C code on the radiochromic film in contact with the plaque, in an area of  $5 \times 5 \text{ cm}^2$ , with a  $0.5 \times 0.5 \text{ cm}^2$  resolution, for the three simulated cases: a) Homogeneous plaque with nominal thickness; b) Heterogeneous plaque divided in four quadrants with different thicknesses; c) Heterogeneous plaque with localized heterogeneities in different areas.

used to make corrections on dose rate values depending on the thickness of each individual plaque. This could be even be used during actual treatment planning.

## 8. Conclusion

The present work described the cold fabrication of the source in plaque form using epoxy resin, paying special attention to factors that can greatly impact dose distribution. MCNP Monte Carlo simulation was used to evaluate the final dose curve.

The fabrication methodology was tested in two molds: commercial silicone and Teflon. The epoxy plaques were manufactured from mixture of the resin SQ2220 and catalyst SQ3154. The proportion was 2: 1 in mass of resin and catalyst, respectively.

The measurements were performed at different points on the plaque, as well as averages and respective standard deviations were calculated. The epoxy plaque fabricated with the silicone mold yield a high degree of variation in thickness uniformity. The Teflon mold presented better agreement.

Average dose obtained by Monte Carlo simulation for the homogeneous plaque was  $16.97 \pm 2.26\%$  cGy/s in the central  $4 \times 4 \text{ cm}^2$  region. Dose in each section of the scored grid at this region varied less than 1.4%, showing good homogeneity at the dose for this size of plaque providing homogeneous thickness is obtained at fabrication.

But the simulation also showed that differences of less than 0.01 cm in thickness within the plaque, which were noted on the actual manufactured plaques, lead to differences of up to 12% in the dose rate, which increases up to 40% if the thickness differs by more than 0.02 cm, also noted on the actual plaques. Although these results are obtained for the plaque simulated in quadrants, therefore expected to be of lesser impact in cases of thickness variation within smaller areas, dose rate was noted to vary as high as 25% for an abrupt variation of 0.02 cm in thickness. This shows how important it is to maintain source thickness homogeneity. Through simulation results, an equation was obtained considering the thickness range of 0.2–0.6 cm. It can be used to estimated variations on dose range for plaques manufactured with different thickness.

Future work includes radiative source manufacture and experimental dosimetry.

## Authors contribution

São Paulo, February 15, 2021. Dear Editor of Applied Radiation and Isotopes The authors contributions for New model for an epoxy-based brachytherapy source to be used in spinal cancer treatment are as follows: José T. Silva Conceptualization; Data curation; Formal analysis;

Investigation; Methodology; Project administration; Validation; Visualization; Writing - original draft Carla DARUICH DE SOUZA, PhD Formal analysis; Investigation; Project administration; Writing - original draft Lucas Verdi Angelocci, mSc Conceptualization; Data curation; Formal analysis; Software; Validation; Visualization; Writing - original draft Wilmmmer Alexander Arcos Rosero, mSc Conceptualization; Data curation; Formal analysis; Validation; Visualization; Roles/Writing - original draft Beatriz Ribeiro Nogueira, mSc Conceptualization; Data curation; Methodology; Validation Ruanyto Willy Correia Carlos Alberto ZEITUNI, PhD Funding acquisition; Project administration; Resources; Supervision; Maria Elisa C. M. ROSTELATO, PhD Formal analysis; Funding acquisition; Project administration; Resources; Supervision; Validation; Thank you, Best Regards. Dr. Carla Daruich de Souza.

## Declaration of competing interest

The authors declare that they have no known competing financial interests or personal relationships that could have appeared to influence the work reported in this paper.

## Acknowledgments

JTS would like to thank: CNEN- Comissão Nacional de Energia Nuclear [grant number 01342.002187/2019–96].

CDS would like to thank: FAPESP- Fundação de Amparo à Pesquisa do Estado de São Paulo, BRAZIL [grant number 2018/18526-2]

LVA would like to thank: CAPES- Coordenação de Aperfeiçoamento de Pessoal de Nível Superior, BRAZIL [grant number 88882.333477/2019-01]; IAEA- International Atomic Energy Agency [grant number BRA 17013]

## References

- Benega, M.G., Nagatomi, H., Rostelato, M.E.C.M., Karan, D.J., Peleias Júnior, F.S., Souza, C.D., Tiezzi, R., Rodrigues, B.T., 2013. Development of Radioactive Sealed Sources in Epoxy matrix., INAC - International Nuclear Atlantic Conference (Recife - Brazil).
- Benega, M.G., Souza, C.D., Rostelato, M.E.C.M., Mattos, F.R., Júnior, F.S.P., Nagatomi, H., Zeituni, C.A., 2012. Desenvolvimento De Fontes Radioativas Seladas Em Matriz Epóxi., Congresso da SBRT (Curitiba - Brazil).
- Bento, R.E., 2011. Estudo do Comportamento da Resina Base na Formulação de Compósitos de Politetrafluoretileno com Bronze, Engenharia Química. Universidade de Campinas, Faculdade de Engenharia Química.
- Blackburn Electric Wires, 2012. SAFETY DATA SHEET: ULTIMEG 2220. <http://www.bew.com.au/files/2220%20msds%20eng.pdf>.
- Briesmeister, J.F., 2002. A General Monte Carlo N-Particle Transport Code, Version 4C. Los Alamos National Laboratory, Radiation Safety Information Computational Center, Oak Ridge, TN.

- Castro, T.C., 2008. Avaliação da resistência ao rasgamento do silicone submetido à ação de suor artificial. Universidade de São Paulo, Faculdade de Odontologia.
- Daruich de Souza, C., Kim, J.J., Hong, J.T., 2021. Start here when performing radiochemical reactions. In: Badria, F.A. (Ed.), Radiopharmaceuticals. InTechOPEN. <https://www.intechopen.com/online-first/77528>.
- Ebnesajjad, S., 2011. 6 - adhesives for medical and dental applications. In: Modjarrad, K., Ebnesajjad, S. (Eds.), Handbook of Polymer Applications in Medicine and Medical Devices. William Andrew Publishing, Oxford, pp. 103–129.
- Ehlers, J.-E., Rondan, N.G., Huynh, L.K., Pham, H., Marks, M., Truong, T.N., 2007. Theoretical study on mechanisms of the Epoxy–Amine curing reaction. *Macromolecules* 40, 4370–4377.
- Folkert, M.R., Bilsky, M.H., Cohen, G.a.N., Voros, L., Oh, J.H., Zaidner, M., Laufer, I., Yamada, Y., 2015. Local recurrence outcomes using the 32P intraoperative brachytherapy plaque in the management of malignant lesions of the spine involving the dura. *Brachytherapy* 14, 202–208.
- Giannotti, M.I., Galante, M.J., Oyanguren, P.A., Vallo, C.I., 2003. Role of intrinsic flaws upon flexural behaviour of a thermoplastic modified epoxy resin. *Polym. Test.* 22, 429–437.
- Gooch, J.W., 2011. Curing agents for epoxy resins. In: Gooch, J.W. (Ed.), *Encyclopedic Dictionary of Polymers*. Springer New York, New York, NY, p. 187.
- Ignatenko, V.Y., Ilyin, S.O., Kostyuk, A.V., Bondarenko, G.N., Antonov, S.V., 2020. Acceleration of epoxy resin curing by using a combination of aliphatic and aromatic amines. *Polym. Bull.* 77, 1519–1540.
- INTERNATIONAL ATOMIC NUCLEAR AGENCY, 2019. Live Chart of Nuclides: Nuclear Structure and Decay Data. <http://www-nds.iaea.org/relnsd/vcharthtml/VChartHTML.html>.
- Konuray, A.O., Fernández-Francos, X., Ramis, X., 2017. Analysis of the reaction mechanism of the thiol–epoxy addition initiated by nucleophilic tertiary amines. *Polym. Chem.* 8, 5934–5947.
- Lam, M., Migonney, V., Falentin-Daudre, C., 2020. Review of silicone surface modification techniques and coatings for antibacterial/antimicrobial applications to improve breast implant surfaces. *Acta Biomater.* 121, 68–88.
- Liravi, F., Toyserkani, E., 2018. Additive manufacturing of silicone structures: a review and prospective. *Add. Manufact.* 24, 232–242.
- Meyerhof, W.E., 1989. *Elements of Nuclear Physics*. McGraw-Hill Book Company, New York.
- Nabors, L.B., Ammirati, M., Bierman, P.J., Brem, H., Butowski, N., Chamberlain, M.C., DeAngelis, L.M., Fenstermaker, R.A., Friedman, A., Gilbert, M.R., Hesser, D., Holdhoff, M., Junck, L., Lawson, R., Loeffler, J.S., Maor, M.H., Moots, P.L., Morrison, T., Mrugala, M.M., Newton, H.B., Portnow, J., Raizer, J.J., Recht, L., Shrieve, D.C., Sills Jr., A.K., Tran, D., Tran, N., Vrionis, F.D., Wen, P.Y., McMillian, N., Ho, M., National Comprehensive Cancer, N., 2013. Central nervous system cancers. *J. Natl. Compr. Canc. Netw. : J. Natl. Compr. Canc. Netw.* 11, 1114–1151.
- National Institute of Standards and Technology, 2020. ESTAR Stopping-Power and Range Tables for Electrons. Physics. [nist.gov](http://nist.gov).
- Oldring, P.K.T., 2003. Coatings, colorants, and paints. In: Meyers, R.A. (Ed.), *Encyclopedia of Physical Science and Technology*, third ed. Academic Press, New York, pp. 175–190.
- Oliveira, M.L., Reis, L.C.O., Leão, R.L.C., Fragoso, M.C.F., Lima, F.R.A., 2020. Solid standards for positron emitters. *Radiat. Phys. Chem.* 167, 108327.
- Palmer, A.L., Dimitriadis, A., Nisbet, A., Clark, C.H., 2015. Evaluation of Gafchromic EBT-XD film, with comparison to EBT3 film, and application in high dose radiotherapy verification. *Phys. Med. Biol.* 60, 8741–8752.
- Pandey, U., Sarma, H.D., Ingle, A.D., Kulloli, B.S., Samuel, G., Venkatesh, M., 2006. Radioactive skin bandages incorporating 32P for treatment of superficial tumors. *Cancer Biother. Radiopharm.* 21, 257–262.
- Podgorsak, E.B., 2005. *Radiation oncology physics: a handbook for teachers and students*. In: International Atomic Energy Agency. Vienna.
- Regine, W.F., Huhn, J.L., Patchell, R.A., St Clair, W.H., Strottmann, J., Meigooni, A., Sanders, M., Young, A.B., 2002. Risk of symptomatic brain tumor recurrence and neurologic deficit after radiosurgery alone in patients with newly diagnosed brain metastases: results and implications. *Int. J. Radiat. Oncol. Biol. Phys.* 52, 333–338.
- Rochester, J.R., Bolden, A.L., 2015. Bisphenol S and F: a systematic review and comparison of the hormonal activity of bisphenol A substitutes. *Environ. Health Perspect.* 123, 643–650.
- Rogers, D., Bazalova-Carter, M., Bolch, W., Heath, E., McNitt-Gray, M., Sempau, J., Williamson, J., 2018. RECORDS: improved reporting of Monte Carlo Radiation transport studies: report of the AAPM Research committee task group 268. *AAPM-Am. Assoc. Phys. Med.* 5. <https://www.aapm.org/pubs/reports/detail.asp?docid=168>.
- Sanborn, G.E., 2006. In: Ryan, S.J., Hinton, D.R., Schachat, A.P., Wilkinson, C.P. (Eds.), Chapter 47 - Circumscribed Choroidal Hemangioma, fourth ed., *Retina*. Mosby, Edinburgh, pp. 829–842.
- Silicone, Shinetsu, 2020. Characteristic Properties of Silicone Rubber Compounds. [https://www.shinetsusilicone-global.com/catalog/pdf/rubber\\_e.pdf](https://www.shinetsusilicone-global.com/catalog/pdf/rubber_e.pdf).
- Tong, W.Y., Folkert, M.R., Greenfield, J.P., Yamada, Y., Wolden, S.L., 2014. Intraoperative phosphorus-32 brachytherapy plaque for multiply recurrent high-risk epidural neuroblastoma. *J. Neurosurg. Pediatr.* 13, 388–392.
- Vandenberg, L.N., 2014. Low-dose effects of environmental chemicals: bisphenol A as a case study. In: Wexler, P. (Ed.), *Encyclopedia of Toxicology*, third ed. Academic Press, Oxford, pp. 111–117.
- Vidil, T., Tournilhac, F., Musso, S., Robisson, A., Leibler, L., 2016. Control of reactions and network structures of epoxy thermosets. *Prog. Polym. Sci.* 62, 126–179.
- Yamada, Y., Lovelock, D.M., Yenice, K.M., Bilsky, M.H., Hunt, M.A., Zatzky, J., Leibel, S. A., 2005. Multifractionated image-guided and stereotactic intensity-modulated radiotherapy of paraspinal tumors: a preliminary report. *Int. J. Radiat. Oncol. Biol. Phys.* 62, 53–61.
- Ziessman, H.A., O'Malley, J.P., Thrall, J.H., 2014. Chapter 12 - Oncology: Non-positron Emission Tomography, *Nuclear Medicine*, fourth ed. W.B. Saunders, Philadelphia, pp. 265–287.